



# Tract Specificity of Age Effects on Diffusion Tensor Imaging Measures of White Matter Health

Stephanie Matijevic\* and Lee Ryan

Cognition and Neuroimaging Laboratory, Department of Psychology, University of Arizona, Tucson, AZ, United States

## OPEN ACCESS

### Edited by:

Annalena Venneri,  
The University of Sheffield,  
United Kingdom

### Reviewed by:

Toshikazu Ikuta,  
University of Mississippi,  
United States  
Jimmy Lätt,  
Lund University, Sweden

### \*Correspondence:

Stephanie Matijevic  
smatijevic@email.arizona.edu

**Received:** 13 November 2020

**Accepted:** 11 February 2021

**Published:** 15 March 2021

### Citation:

Matijevic S and Ryan L (2021) Tract Specificity of Age Effects on Diffusion Tensor Imaging Measures of White Matter Health. *Front. Aging Neurosci.* 13:628865. doi: 10.3389/fnagi.2021.628865

Well-established literature indicates that older adults have poorer cerebral white matter integrity, as measured through diffusion tensor imaging (DTI). Age differences in DTI have been observed widely across white matter, although some tracts appear more sensitive to the effects of aging than others. Factors like APOE  $\epsilon$ 4 status and sex may contribute to individual differences in white matter integrity that also selectively impact certain tracts, and could influence DTI changes in aging. The present study explored the degree to which age, APOE  $\epsilon$ 4, and sex exerted global vs. tract specific effects on DTI metrics in cognitively healthy late middle-aged to older adults. Data from 49 older adults (ages 54–92) at two time-points separated by approximately 2.7 years were collected. DTI metrics, including fractional anisotropy (FA) and mean diffusivity (MD), were extracted from nine white matter tracts and global white matter. Results showed that across timepoints, FA and MD increased globally, with no tract-specific changes observed. Baseline age had a global influence on both measures, with increasing age associated with lower FA and higher MD. After controlling for global white matter FA, age additionally predicted FA for the genu, callosum body, inferior fronto-occipital fasciculus (IFOF), and both anterior and posterior cingulum. Females exhibited lower global FA on average compared to males. In contrast, MD was selectively elevated in the anterior cingulum and superior longitudinal fasciculus (SLF), for females compared to males. APOE  $\epsilon$ 4 status was not predictive of either measure. In summary, these results indicate that age and sex are associated with both global and tract-specific alterations to DTI metrics among a healthy older adult cohort. Older women have poorer white matter integrity compared to older men, perhaps related to menopause-induced metabolic changes. While age-related alterations to white matter integrity are global, there is substantial variation in the degree to which tracts are impacted, possibly as a consequence of tract anatomical variability. The present study highlights the importance of accounting for global sources of variation in DTI metrics when attempting to investigate individual differences (due to age, sex, or other factors) in specific white matter tracts.

**Keywords:** aging, diffusion tensor imaging, white matter, MRI, sex

## INTRODUCTION

Cerebral white matter undergoes multiple changes throughout healthy aging. Dysmyelination, axonal degeneration, ischemia, and inflammatory processes associated with aging may compromise the structural integrity of axonal fibers within cerebral white matter bundles (Peters, 2009). The overall impact of these various pathological processes on white matter microstructure can be indirectly assessed through the use of diffusion tensor imaging (DTI; Alexander et al., 2007). Based on the principle that intact myelinated fibers restrict the movement of water within and especially across fiber bundles, DTI derives estimates of diffusion magnitude and directionality that can serve as proxies for white matter microstructural integrity. The DTI-derived metric mean diffusivity (MD) expresses the average amount of diffusion occurring within an image voxel. Fractional anisotropy (FA) is a ratio reflecting the directional consistency of diffusion, with higher values indicating that diffusion within a voxel is primarily restricted to one direction or, in cases like crossing fibers, to two directions (O'Donnell and Westin, 2011). When calculated for voxels containing white matter tissue, both MD and FA are influenced by attributes of individual axons and fiber bundles or tracts, such as the density of myelin and tract compactness, as well as the size and composition of extracellular components (Alexander et al., 2007). Opposing correlations are typically seen between these measures and age in adulthood. Increasing age is typically associated with higher MD and lower FA (Lebel et al., 2012; Cox et al., 2016; Storsve et al., 2016; for review, see Madden et al., 2009), likely reflecting the impact of a combination of age-related phenomena including dysmyelination, glial-induced inflammatory activity, dysfunctional glial clearance of extracellular debris, axonal degeneration, and ischemic injury (Peters, 2009; Raj et al., 2017; Chapman and Hill, 2020).

Axial diffusivity (AD) and radial diffusivity (RD) are additional DTI metrics that may correlate more specifically to certain types of white matter pathology. AD represents diffusion occurring along the length of white matter fibers, while RD is calculated as the amount of diffusion perpendicular to the main directional axis of fibers. Early studies of optic nerve fiber damage (Song et al., 2003, 2005) indicated that increases in AD and RD values correlate with axonal degradation and dysmyelination, respectively. However, a more diverse set of animal models for multiple sclerosis (Budde et al., 2007, 2009; Falangola et al., 2014) and spinal cord injury (Budde et al., 2007) have revealed that AD is less specific for axonal degradation and RD is less specific for dysmyelination when multiple pathologies co-occur (for review, see Winklewski et al., 2018). Human studies have consistently noted increases in RD associated with increasing age in late adulthood (Bennett et al., 2010; Brickman et al., 2012; Marstaller et al., 2015), while the relationship between age and AD is less straightforward, as both increases and decreases in AD have been demonstrated among older adults (Bennett et al., 2010; Burzynska et al., 2010).

A long-standing question regarding cerebral white matter abnormalities in aging is the degree to which these changes can be characterized as uniform across the brain vs. regionally specific.

Twin studies have revealed that genetics account for over half of the global variation in DTI metrics within middle-aged to older adults (Vuoksimaa et al., 2017; Gustavson et al., 2019), as well as additional tract-specific variation in late adulthood (Kanchibhotla et al., 2014; Vuoksimaa et al., 2017; Hatton et al., 2018; Gustavson et al., 2019). Gustavson et al. (2019) noted that these findings emphasize the importance of accounting for global sources of variation in white matter DTI values when attempting to examine associations between individual tracts and variables like age. Multivariate analyses of white matter tract DTI values have identified a general factor of white matter integrity capable of explaining a substantial amount of variance shared across tracts, among older adults (Penke et al., 2010; Lövdén et al., 2013; Cox et al., 2016). Cox et al. (2016) demonstrated an association between age and a general factor for FA, derived through the latent-variable analysis of tract FA values. However, this general factor did not fully account for tract-specific age associations, indicating regional variation in the magnitude of the association between age and FA. Such regional variation has been observed within the corpus callosum, as the anterior segment of the corpus callosum tends to be more sensitive to age-related FA reductions compared to posterior segments (Bendlin et al., 2010; Michielse et al., 2010; Bennett et al., 2010; Cox et al., 2016). Overall, the corpus callosum tends to show smaller alterations to both FA and MD compared to long-range association tracts (such as the superior longitudinal, inferior longitudinal, inferior fronto-occipital, and uncinate fasciculi) and limbic tracts (fornix and cingulum), but larger alterations compared to sensorimotor projection tracts such as the internal capsule (de Groot et al., 2015; Hoagey et al., 2019). However, it is important to note that tract-specific changes in white matter are inconsistent across studies. For instance, while an anterior-to-posterior gradient of age-related FA reduction has been consistently noted within the corpus callosum, there is mixed evidence as to whether this gradient applies to other regions of cerebral white matter (Brickman et al., 2012; Hoagey et al., 2019).

Genetics, lifestyle, and health factors may contribute to individual differences in white matter integrity, particularly in later life (Bender and Raz, 2015). Apolipoprotein E (APOE)  $\epsilon 4$  allele, the strongest known genetic risk factor for the development of sporadic Alzheimer's disease (Kline, 2012), has been shown to impact DTI metrics in older adults. Cross-sectional studies have noted that cognitively healthy older adults carrying one or more copies of the  $\epsilon 4$  allele show greater DTI alterations compared to non-carriers, particularly in FA (for review, see Kanchibhotla et al., 2013). Among older adults,  $\epsilon 4$  is associated with reduced FA in specific tracts including the cingulum (Smith et al., 2010; Lyall et al., 2014; Cavedo et al., 2017), the corpus callosum (Persson et al., 2006; Smith et al., 2010; Laukka et al., 2015; Cavedo et al., 2017), and the superior and inferior longitudinal fasciculi (Smith et al., 2010; Lyall et al., 2014; Cavedo et al., 2017). However, multiple other studies have reported the absence of an  $\epsilon 4$  effect for any white matter tract (Bendlin et al., 2010; Westlye et al., 2012; Ly et al., 2014; Nyberg and Salami, 2014). One explanation for these contradictory findings is that  $\epsilon 4$  might influence the

trajectory of age-related changes in DTI metrics, rather than engendering an overall difference between  $\epsilon 4$  carriers and non-carriers. Supporting this idea, a cross-sectional study by Ryan et al. (2011) reported an interaction between  $\epsilon 4$  status and age in a cohort of older adults, ages 52–92. They found that  $\epsilon 4$  carriers exhibited steeper age-related increases in the average diffusion coefficient across all white matter regions, and steeper FA decreases within frontal white matter, temporal white matter, and the genu of the corpus callosum compared to non-carriers. Similar findings of an  $\epsilon 4$  by age interaction have been noted in other studies (Adluru et al., 2014; Williams et al., 2019), although some studies have not detected such an interaction (Nyberg and Salami, 2014; Rieckmann et al., 2016).

While APOE  $\epsilon 4$  has been the focus of multiple studies, other potentially important factors, such as sex, have garnered relatively little attention. Middle-aged females undergo sweeping endocrine changes during menopause that likely contribute to increased prevalence of autoimmune diseases (Desai and Brinton, 2019) and potentially greater susceptibility to age-related white matter damage through enhanced dysmyelination (Klosinski et al., 2015). Indeed, a poor metabolic profile in combination with the APOE  $\epsilon 4$  genotype has been associated with reduced cognitive performance in otherwise healthy postmenopausal women (Karim et al., 2019). Mosconi et al. (2017) examined white matter volumes for pre-, peri- and post-menopausal middle-aged women and found a significant decline in white matter volume from pre- to post-menopausal stages, providing support for the idea that menopause contributes to white matter degeneration in older women. Sex differences in white matter may also be present from birth, however, as suggested by research demonstrating an influence of sex hormones on white matter development in adolescence (Herting et al., 2012; Menzies et al., 2015; Peper et al., 2015; Ho et al., 2020). Sexual dimorphism in DTI metrics has not been consistently observed in adults, but studies that have found sex differences note that females tend to have lower FA compared to males (Lebel et al., 2010; Inano et al., 2011; van Hemmen et al., 2017; Ritchie et al., 2018), although others have reported the opposite pattern as well (O'Dwyer et al., 2012). In part, this inconsistency could stem from regional variability in the impact of sex on DTI metrics. For example, Inano et al. (2011) reported age-related changes in global measures of FA, AD, and RD, but found sex differences that were tract-specific. Significantly lower FA was observed in females compared with males in multiple regions including the splenium of the corpus callosum, the posterior internal capsule, bilateral cingulum, and bilateral superior longitudinal fasciculus (but note that FA was higher for females in the columns of the fornix). The possibility that menopause may enhance susceptibility to white matter damage, particularly in a tract-specific manner, highlights the importance of considering sex differences in DTI studies of aging.

The present study sought to characterize the degree to which age,  $\epsilon 4$  status, and sex influence white matter integrity among older adults, and whether these differences are best characterized as global or tract-specific. DTI metrics were obtained from whole-brain white matter maps as well as tracts

commonly implicated in studies of aging, including the genu, body, and splenium of the corpus callosum, the anterior and posterior cingulum bundles, the superior longitudinal fasciculi, the inferior fronto-occipital fasciculi, the fornix, and the uncinate fasciculi. Additionally, we obtained these DTI measures from our cohort at two time-points separated 2.7 years apart on average. Cross-sectional studies are limited in their ability to precisely characterize the impact of aging on white matter integrity. While longitudinal studies have generally demonstrated age-related changes to FA and MD that are similar to cross-sectional findings (Teipel et al., 2010; Sexton et al., 2014; Bender and Raz, 2015; Bender et al., 2016; Williams et al., 2019), they have also identified white matter changes that are not detected in cross-sectional studies. For example, Bender and Raz (2015) found increases in FA across a two to three year period in the body of the corpus callosum, in contrast to cross-sectional FA decreases with age in this tract at baseline. Examining how DTI metrics shift over time may provide a more precise assessment of global and tract-specific effects of risk factors on white matter integrity.

## MATERIALS AND METHODS

### Participants

Forty-nine cognitively healthy older adults (ages 54–92) who participated in Ryan et al. (2011) were recruited for a second wave of data collection approximately 2.7 years after their first visit (see **Table 1** for demographics). All participants were community-dwelling residents of the Tucson, Arizona region. Eligible participants were screened for neurological disorders, drug/alcohol abuse, psychiatric disorders, stroke, traumatic brain injury, and MRI complications, and scored within normal limits on a neuropsychological test battery assessing memory, executive functions, and processing speed. Informed consent was obtained following the guidelines set by the University of Arizona's Institutional Review Board.

### APOE Genotyping

Saliva samples were obtained *via* the Oragene-DNA device (OG-500, DNA Genotek Inc., Toronto, ON, Canada) from participants and sent to the Translational Genomics Research Institute (Phoenix, AZ, USA) for genotyping. DNA was extracted from the saliva samples using the manufacturer's protocol and genotyped for two single nucleotide polymorphisms within APOE, rs429358, and rs7412, *via* TaqMan chemistry (Thermo

**TABLE 1** | Sample demographics.

| Demographic variable                      |                            |
|---|----------------------------|
| <i>N</i>                                  | 49                         |
| Years of age at T1, mean $\pm$ SD (range) | 70.4 $\pm$ 8.2 (54.1–91.8) |
| Months between scans, mean $\pm$ SD       | 32.9 $\pm$ 6.63            |
| Sex, <i>N</i> (%)                         |                            |
| Male                                      | 13 (27%)                   |
| Female                                    | 36 (73%)                   |
| Years of education, mean $\pm$ SD         | 16.0 $\pm$ 2.6             |
| $\epsilon 4$ Status, <i>N</i> (%)         |                            |
| $\epsilon 4$ Carrier                      | 20 (41%)                   |
| $\epsilon 4$ Non-carrier                  | 29 (59%)                   |

Fisher Scientific Inc., Waltham, MA, USA). Participants with the  $\epsilon 2/\epsilon 4$ ,  $\epsilon 3/\epsilon 4$ , or  $\epsilon 4/\epsilon 4$  genotype were categorized as  $\epsilon 4$  carriers ( $n = 20$ ) for this study, while  $\epsilon 2/\epsilon 3$  and  $\epsilon 3/\epsilon 3$  individuals were considered non-carriers ( $n = 29$ ). No  $\epsilon 2$  homozygotes were present in this sample.

## MR Image Acquisition

At both visits, images were obtained with a General Electric 3.0 T Signa (Milwaukee, WI, USA) MR scanner. An echo-planar DTI sequence was used to collect two non-diffusion weighted images and diffusion-weighted images in 25 directions ( $b$ -value = 1,000  $s/mm^2$ , 58 contiguous axial sections, 2.6 mm thickness, TE = 71 ms, TR = 13,000 ms, matrix =  $96 \times 96$ , FOV =  $250 \times 250$   $mm^2$ , voxel size = 2.6  $mm^3$ ). High resolution T1-weighted SPGR images were obtained with the following parameters: 0.7 mm thickness, TE = 2 ms, TR = 5.1 ms, flip angle =  $15^\circ$ , matrix =  $256 \times 256$ , FOV =  $260 \times 260$   $mm^2$ . Participants with incidental MR findings, such as evidence of past stroke damage, were excluded from the study.

## Diffusion Tensor Imaging

Diffusion-weighted images were visually inspected for artifacts. Skull stripping, motion and eddy current corrections, and tensor fitting were performed with FSL tools<sup>1</sup> (Smith et al., 2004). Registration of images across the two time-points followed an optimized longitudinal DTI analysis protocol detailed in Keihaninejad et al. (2013), which was developed to track white matter changes occurring in neurodegenerative conditions such as Alzheimer's disease. Keihaninejad et al.'s (2013) protocol attempts to mitigate the sensitivity of ROI-based analyses to registration and partial volume errors, which are particularly an issue when atrophy is present, by incorporating diffusion tensor information into the registrations such that the alignment process takes into account local fiber orientation. Using DTI-TK's<sup>2</sup> tensor-based registration method (Zhang et al., 2006), a within-subject template was created for each participant by registering and averaging the tensor images from both time points. Within-subject templates from all participants were averaged together to create a group template, and each participant's two tensor images were then normalized to this group template.

For each participant, FA, MD, RD AD maps were derived from the normalized tensor images. To extract tract-specific DTI metrics, the Johns Hopkins University ICBM-DTI-81 2 mm white matter atlas (JHU atlas; Mori et al., 2008) was registered to the study-specific group template. The JHU atlas tract labels were then used to identify regions of interest (ROIs) on the normalized DTI maps for each participant. The ROIs were further masked with a binary white matter mask created by thresholding the FA maps at a value of 0.2 to ensure that only fully-volumed white matter was included in the ROIs. ROIs (see **Figure 1**) included the anterior cingulum, posterior cingulum, superior longitudinal fasciculus (SLF), inferior fronto-occipital fasciculus (IFOF), fornix body, uncinate fasciculus, and the corpus callosum. The corpus callosum was segmented into the

genus, callosal body, and splenium, defined in the JHU atlas as the first, second, and last thirds of the corpus callosum, respectively. The IFOF ROI comprised of the temporal and occipital portions of the tract and was inclusive of the inferior longitudinal fasciculus. FA, MD, RD, and AD values were averaged across all voxels within an ROI. For bilateral ROIs (anterior and posterior cingulum, SLF, uncinate fasciculus, and IFOF), values were extracted separately, then averaged across the left and right ROIs, since we did not have *a priori* hypotheses regarding laterality effects. Additionally, we found that the values from left and right hemispheres for each tract at baseline were correlated at  $r = 0.35$  or higher, all  $p$ 's < 0.05. To calculate global diffusion measures, the white matter mask was applied to each DTI map—FA, MD, RD, and AD—and the values for all voxels within the mask were then averaged.

## Statistical Analyses

To determine whether the impact of the independent variables on DTI metrics are best characterized as global or tract-specific, we compared the outcomes from two sets of mixed factor MANOVAs, with and without the inclusion of global DTI measures as covariates. This allowed us to calculate the difference in variance explained within specific tracts that was accounted for by our predictors before and after controlling for global DTI measures. Employing MANOVAs also allowed us to control for experiment-wise error due to the large numbers of tracts included in the study.

First, separate MANOVAs were conducted to predict DTI values within specific tracts, without controlling for global DTI measures. Diffusion values at time 1 and time 2 for each tract were entered as dependent variables, with time (time 1, time 2) modeled as a within-subject predictor. Mean-centered age at time point 1, sex (female, male), and APOE  $\epsilon 4$  status (carrier, non-carrier) were included as between-subject predictors. All main effects and the interactions between time and the between-subject predictors were included in the model. Pillai's Trace served as the test statistic in the MANOVA models, as it is more robust to inhomogeneity of covariance and variance. The second set of MANOVA models were identical to the first set but controlled for global sources of variation in DTI metrics, through the inclusion of the global DTI measures (at time 1) to their respective models as a covariate. The two sets of models were compared to identify associations with tract-specific DTI values that were independent of global white matter influences.

As a follow-up analysis for each effect identified as tract-specific, stepwise regressions were conducted for each tract. Global FA or MD was entered as a predictor into each regression model first, followed by the predictor of interest. To further explore associations between our predictors and global DTI measures, we conducted mixed factor ANOVAs. These models included the same set of predictors as the tract-specific MANOVAs—the age at time 1 (mean-centered), sex, APOE  $\epsilon 4$  status, time, and the interactions between time and each between-subject variable. In the two separate ANOVAs, global FA and global MD at time 1 and time 2 were entered as dependent variables.

<sup>1</sup><http://fsl.fmrib.ox.ac.uk>

<sup>2</sup><http://dti-tk.sourceforge.net>

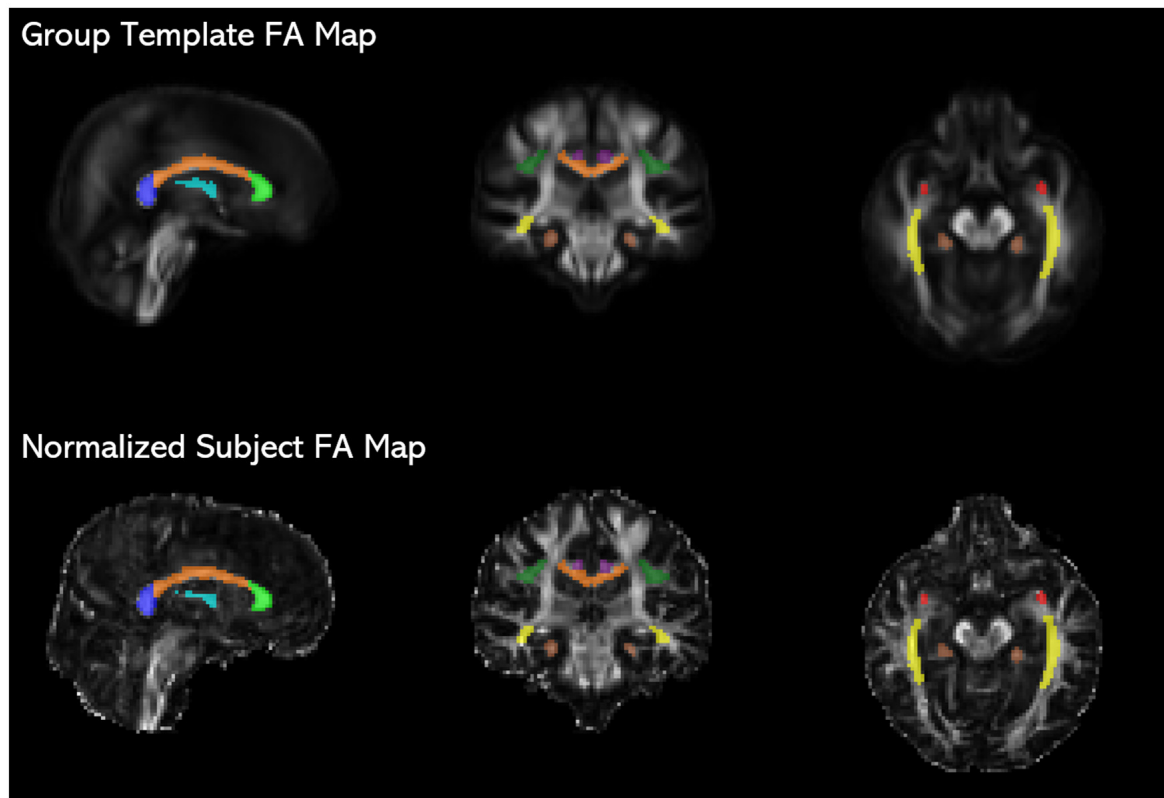


**FIGURE 1 |** JHU ICBM-DTI-81 white matter atlas tract labels (Mori et al., 2008) registered to the study-specific group template are overlaid on fractional anisotropy (FA) maps of the group template and an individual subject's time 1 image normalized to the group template space, showing the placement of the fornix (light blue), genu (light green), corpus callosum body (orange), splenium (blue), uncinate fasciculus (red), inferior fronto-occipital fasciculus (IFOF; yellow), anterior cingulum (purple), posterior cingulum (brown), and superior longitudinal fasciculus (SLF; dark green).

## RESULTS

Correlations amongst global MD, RD, and AD values at time point 1 yielded Pearson  $r$  coefficients greater than 0.9, while correlations between these measures and global FA were smaller with coefficients ranging between 0.4 and 0.7 (see **Table 2**). The strong correlations between AD, RD, and MD values suggested that these measures were redundant. Thus, only MD and FA values were included in our analyses.

### Determining Tract-Specific Predictors of DTI Metrics

To determine whether the impact of the independent variables on DTI metrics are best characterized as global or tract-specific, we compared the outcomes from two sets of mixed factor

MANOVAs, with and without the inclusion of global DTI measures as covariates. This allowed us to calculate the difference in variance explained within specific tracts that was accounted for by our predictors before and after controlling for global DTI measures. Employing MANOVAs also allowed us to control for experiment-wise error due to the large numbers of tracts included in the study.

First, separate MANOVAs were conducted to predict FA and MD values within specific tracts, without controlling for global DTI measures. Diffusion values at time 1 and time 2 for each tract were entered as dependent variables, with time (time 1, time 2) modeled as a within-subject predictor. Mean-centered age at time point 1, sex (female, male), and APOE  $\epsilon 4$  status (carrier, non-carrier) were included as between-subject predictors. All main effects and the interactions between time and the between-subject predictors were included in the model. Pillai's Trace served as the test statistic in the MANOVA models, as it is more robust to inhomogeneity of covariance and variance. The second set of MANOVA models were identical to the first set but controlled for global sources of variation in DTI metrics. Global FA and MD values at time 1 were added to the models as covariates for FA and MD values, respectively. The two sets of models were compared to identify associations

**TABLE 2 |** Correlation matrix showing Pearson  $r$  values for associations between global diffusion tensor imaging (DTI) measures at time point 1.

|           | Global FA | Global RD | Global AD |
|-----------|-----------|-----------|-----------|
| Global RD | -0.685**  |           |           |
| Global AD | -0.432**  | 0.932**   |           |
| Global MD | -0.595**  | 0.989**   | 0.975**   |

\*\* $p < 0.01$ .

**TABLE 3** | Results of the mixed MANOVAs for tract fractional anisotropy (FA) values.

| Predictors             | Tract FA model |        |                | Tract FA model (controlling for Global FA) |        |                |
|------------------------|----------------|--------|----------------|--|--------|----------------|
|                        | F              | p      | Pillai's trace | F  | p      | Pillai's trace |
| <b>Within-subject</b>  |                |        |                |  |        |                |
| Time                   | 2.73           | 0.015  | 0.40           | 1.25                                       | n.s.   | 0.24           |
| Time * Age             | 2.11           | n.s.   | 0.34           | 1.63                                       | n.s.   | 0.29           |
| Time * Sex             | 1.39           | n.s.   | 0.25           | 1.41                                       | n.s.   | 0.26           |
| Time * APOE ε4         | 0.43           | n.s.   | 0.10           | 0.42                                       | n.s.   | 0.10           |
| Time * Global FA       |                |        |                | 1.27                                       | n.s.   | 0.24           |
| <b>Between-subject</b> |                |        |                |  |        |                |
| Age                    | 6.34           | <0.001 | 0.61           | 4.43                                       | 0.001  | 0.53           |
| Sex                    | 3.47           | 0.003  | 0.46           | 1.67                                       | n.s.   | 0.29           |
| APOE ε4                | 1.36           | n.s.   | 0.25           | 1.34                                       | n.s.   | 0.25           |
| Global FA              |                |        |                | 9.61                                       | <0.001 | 0.71           |

On the left, results for the initial version of the model without controlling for global FA are shown. On the right, results for the model controlling for global FA (at time 1) are shown.

**TABLE 4** | Results of the mixed MANOVAs for tract mean diffusivity (MD) values.

| Predictors             | Tract MD model |        |                | Tract MD model (controlling for Global MD) |        |                |
|------------------------|----------------|--------|----------------|--|--------|----------------|
|                        | F              | p      | Pillai's trace | F  | p      | Pillai's trace |
| <b>Within-subject</b>  |                |        |                |  |        |                |
| Time                   | 2.77           | 0.014  | 0.40           | 1.07                                       | n.s.   | 0.21           |
| Time * Age             | 1.51           | n.s.   | 0.27           | 1.56                                       | n.s.   | 0.28           |
| Time * Sex             | 1.45           | n.s.   | 0.26           | 1.53                                       | n.s.   | 0.28           |
| Time * APOE ε4         | 0.73           | n.s.   | 0.15           | 0.73                                       | n.s.   | 0.15           |
| Time * Global MD       |                |        |                | 1.08                                       | n.s.   | 0.21           |
| <b>Between-subject</b> |                |        |                |  |        |                |
| Age                    | 6.10           | <0.001 | 0.60           | 1.43                                       | n.s.   | 0.26           |
| Sex                    | 7.62           | <0.001 | 0.65           | 6.63                                       | <0.001 | 0.62           |
| APOE ε4                | 1.85           | n.s.   | 0.31           | 1.91                                       | n.s.   | 0.32           |
| Global MD              |                |        |                | 11.46                                      | <0.001 | 0.74           |

On the left, results for the initial version of the model without controlling for global MD are shown. On the right, results for the model controlling for global MD (at time 1) are shown.

**TABLE 5** | Pearson correlation  $r$  values for associations between age and tract FA values at time 1.

| Genu    | Callosum body | Splenium | Fornix | Ant. cingulum | Post. cingulum | SLF   | IFOF    | Uncinate |
|---------|---------------|----------|--------|---------------|----------------|-------|---------|----------|
| -0.57** | -0.55**       | -0.40**  | -0.37* | -0.50**       | -0.54**        | -0.22 | -0.48** | -0.31*   |

\*\* $p < 0.01$ ; \* $p < 0.05$ .

with tract-specific DTI values that were independent of global white matter influences. Results from the four mixed factor MANOVAs as well as appropriate follow-up analyses for specific tracts are described below.

### Fractional Anisotropy

Results of the MANOVAs predicting FA are found in **Table 3**. The tract-specific MANOVA without controlling for global FA indicated significant main effects of time, sex, and age. After controlling for global FA at time 1, the main effects of time and sex were no longer significant. The effect of age, however, remained significant. FA values were not significantly influenced by APOE ε4 status in either model, and the interactions between time and other predictor variables did not approach significance in either model.

### Mean Diffusivity

Results of the MANOVAs predicting MD are found in **Table 4**. The tract-specific MANOVA without controlling for global MD showed a similar pattern to FA, indicating the main effects of time, sex, and age. After controlling for global MD, the effect of

time was no longer significant. Unlike the results for FA, the main effect of age also became non-significant, while the main effect of sex remained significant. In both models, and consistent with the results for FA, APOE ε4 status did not predict MD values, and the interactions between time and other predictor variables did not approach significance.

### Tract-Specific Associations Between Age and FA

The MANOVAs indicated that age did not predict MD in specific tracts once global MD was accounted for. However, age predicted FA in specific tracts, even after controlling for global FA. To further explore the effect of age on tract-specific FA values, we first performed Pearson correlations between tract FA values and age at time 1, which showed that increasing age was associated with lower FA in all tracts except for the SLF (see **Table 5**). Stepwise regressions were then performed for each tract in which global FA at time 1 was entered first as a predictor, followed by age at time 1. Results listed in **Table 6**, indicated a negative influence of age on FA values in

**TABLE 6** | Results for stepwise regressions performed on tract FA values (at time 1).

| Tract              | Predictors | $\beta$      | $t$          | $p$              | $F_{(2,46)}$ | Adj. $R^2$  | $R^2$ change |
|--------------------|------------|--------------|--------------|------------------|--------------|-------------|--------------|
| Genu               | Global FA  | 0.55         | 5.51         | <0.001           | <b>33.90</b> | <b>0.58</b> | <b>0.13</b>  |
|                    | <b>Age</b> | <b>-0.38</b> | <b>-3.85</b> | <b>&lt;0.001</b> |              |             |              |
| Callosum body      | Global FA  | 0.39         | 3.30         | 0.002            | <b>18.03</b> | <b>0.42</b> | <b>0.16</b>  |
|                    | <b>Age</b> | <b>-0.42</b> | <b>-3.57</b> | <b>&lt;0.001</b> |              |             |              |
| Splenium           | Global FA  | 0.55         | 4.60         | <0.001           | 16.85        | 0.40        | 0.04         |
|                    | Age        | -0.21        | -1.74        | n.s.             |              |             |              |
| Fornix             | Global FA  | 0.39         | 2.87         | 0.006            | 8.35         | 0.23        | 0.05         |
|                    | Age        | -0.24        | -1.75        | n.s.             |              |             |              |
| Anterior cingulum  | Global FA  | 0.63         | 6.37         | <0.001           | <b>34.51</b> | <b>0.58</b> | <b>0.07</b>  |
|                    | <b>Age</b> | <b>-0.28</b> | <b>-2.81</b> | <b>0.007</b>     |              |             |              |
| Posterior cingulum | Global FA  | 0.18         | 1.42         | n.s.             | <b>10.64</b> | <b>0.29</b> | <b>0.20</b>  |
|                    | <b>Age</b> | <b>-0.47</b> | <b>-3.63</b> | <b>0.001</b>     |              |             |              |
| SLF                | Global FA  | 0.87         | 10.38        | <0.001           | 57.92        | 0.70        | 0.01         |
|                    | Age        | 0.08         | 0.91         | n.s.             |              |             |              |
| IFOF               | Global FA  | 0.62         | 5.96         | <0.001           | <b>30.14</b> | <b>0.55</b> | <b>0.06</b>  |
|                    | <b>Age</b> | <b>-0.27</b> | <b>-2.61</b> | <b>0.012</b>     |              |             |              |
| Uncinate           | Global FA  | 0.52         | 4.00         | <0.001           | 11.17        | 0.30        | 0.01         |
|                    | Age        | -0.13        | -0.99        | n.s.             |              |             |              |

Global FA was entered into each model first, followed by age. Only results for the complete model (Global FA + Age) are included here. Standardized  $\beta$  coefficients,  $t$ -statistics, and  $p$ -values are shown for Global FA and Age predictors. The model-level  $F$  statistic and Adj.  $R^2$  are also reported.  $R^2$  change represents the amount of variance additionally explained in the model after adding Age as a predictor. Statistically significant age effects are bolded.

the genu, callosum body, anterior cingulum, posterior cingulum, and the IFOF that went beyond individual baseline differences in global FA. The additional variance explained by age beyond global FA ranged from 6% in the IFOF to 20% in the posterior cingulum. **Figure 2** depicts the relationships, for these five tracts, between age and tract FA values residualized for global FA values at time 1.

## Tract-Specific Sex Differences in MD Values

In contrast to age, sex did not predict tract-specific FA values once global FA was accounted for, but remained a significant predictor of tract-specific MD values, even after controlling for global MD at time 1. To further explore the association between sex and MD in specific tracts, stepwise regressions were conducted for each tract. Global MD at time 1 was entered as a predictor into each regression model first, followed by sex. Results listed in **Table 7** indicated that MD was higher for females compared to males in the anterior cingulum and SLF (depicted in **Figure 3**). After accounting for global MD, sex increased the variance explained by 16% and 15%, respectively, in these two regions. Although the stepwise regression also showed a significant effect of sex in the genu, we note that this effect did not remain significant after excluding a single outlier.

## Global FA and MD

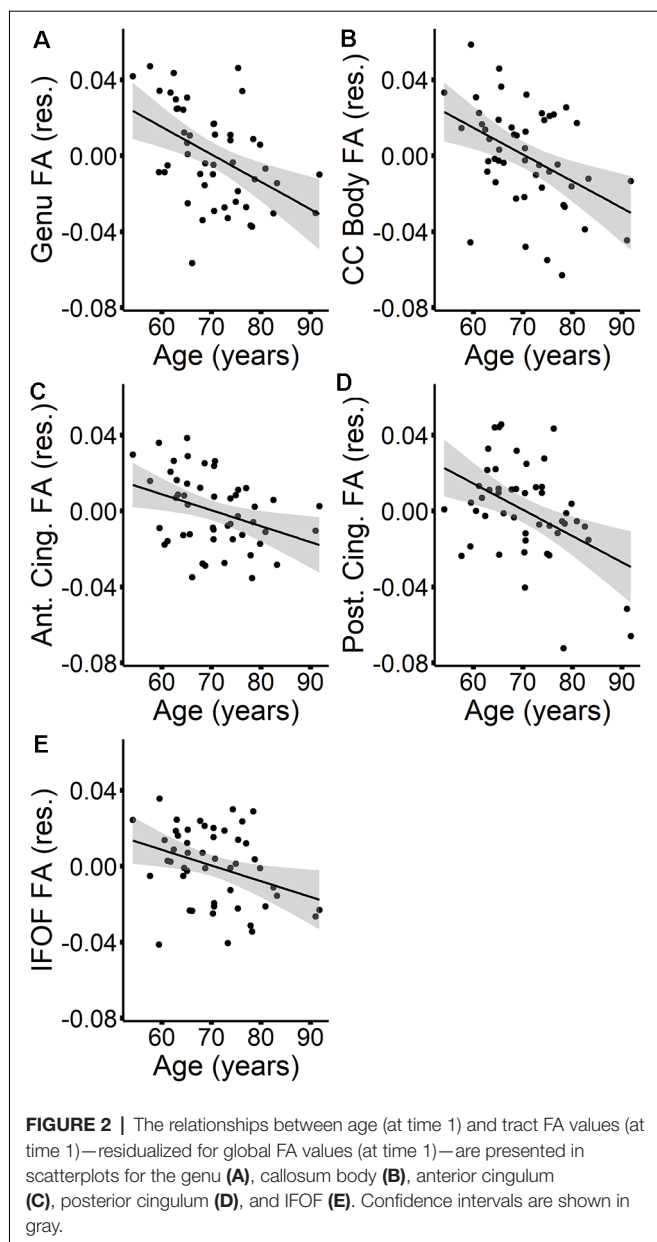
The results of the MANOVAs suggested that the effects of most, but not all, of the independent predictors on tract-specific DTI measures were accounted for, once a global DTI metric was included as a covariate. We therefore conducted two additional mixed factor ANOVAs to better understand the relationship between global DTI metrics and the independent variables. These models included the same set of predictors as the tract-specific MANOVAs—age at

time 1 (mean-centered), sex, APOE  $\epsilon 4$  status, time, and the interactions between time and each between-subject variable. In the two separate ANOVAs, global FA and global MD at time 1 and time 2 were entered as the dependent variables.

The results are listed in **Table 8**. Results indicated a main effect of time on both global FA and global MD (see **Figure 4**). Follow-up paired  $t$ -tests revealed that global MD values were higher at the second time point ( $t_{(48)} = -4.79$ ,  $p < 0.001$ ). Unexpectedly, FA values were also higher at the second time point compared to time 1 ( $t_{(48)} = -3.33$ ,  $p = 0.002$ ). Age at time 1 also predicted global FA and global MD values (see **Figure 5**). Correlations between age at time 1 and global measures at time 1 showed lower global FA values ( $r = -0.35$ ,  $p = 0.015$ ) and higher global MD values ( $r = 0.67$ ,  $p < 0.001$ ) as age increased. Sex predicted global FA and showed a marginal effect on global MD ( $p = 0.051$ ). Males showed higher global FA values at time 1 compared to females ( $t_{(47)} = 3.14$ ,  $p = 0.003$ ; see **Figure 6**). APOE  $\epsilon 4$  status did not predict either global measure, and none of the interaction effects between time and other independent variables approached significance.

## DISCUSSION

In this study, we investigated the influence of age, APOE  $\epsilon 4$  status, and sex on white matter microstructure by examining changes in DTI metrics across two time-points separated by an average of 2.7 years. We sought to clarify the extent to which associations between our variables of interest and DTI metrics are best characterized as global or tract-specific. The results of this study provide evidence of a complex pattern of global and tract-specific white matter differences influenced by time, baseline age, and sex, but not APOE  $\epsilon 4$  status, on FA and MD metrics. These relationships are discussed in detail in the following sections.



## APOE $\epsilon 4$ Did Not Predict FA or MD

We did not observe differences between APOE  $\epsilon 4$  carriers and non-carriers in either tract-specific or global measures of FA and MD. This result is in contrast to evidence from cross-sectional (Persson et al., 2006; Smith et al., 2010; Heise et al., 2011; Lyall et al., 2014; Laukka et al., 2015; Cavado et al., 2017) and longitudinal studies (Williams et al., 2019) linking APOE  $\epsilon 4$  to reduced FA and increased MD values in white matter tracts, particularly those connecting frontal, temporal and parietal regions. However, other studies have failed to find an association with  $\epsilon 4$  (Nyberg and Salami, 2014; Bendlin et al., 2010; Westlye et al., 2012; Ly et al., 2014; Rieckmann et al., 2016), suggesting that the relationship between APOE  $\epsilon 4$  and DTI metrics is likely subtle. It is important to note that our participants were a subset of the cohort included in

Ryan et al. (2011), who found cross-sectional differences in white matter FA and apparent diffusion coefficient (equivalent to MD) values between  $\epsilon 4$  carriers and non-carriers in a larger sample of 126 participants, ages 52–92. The relationship to  $\epsilon 4$  status was dependent on age, however, such that  $\epsilon 4$  differences were more apparent at the older end of the age range. The notion that the effects of APOE  $\epsilon 4$  become more obvious in late adulthood is consistent with the resource modulation hypothesis of genetic influences on aging (Lindenberger et al., 2008; Papenberg et al., 2015). By this view, age-associated losses in neurochemical or anatomical “brain resources” can strengthen genetic influences on cognition and brain structure/function. Thus, studies with larger sample sizes and wider age ranges may be necessary to detect the synergistic effects of age and  $\epsilon 4$  on white matter microstructure. Larger sample sizes would also enable comparison of  $\epsilon 4$  heterozygotes and homozygotes, and thus an exploration of potential dose-dependent effects of the APOE  $\epsilon 4$  allele on white matter.

## Sex Predicted Global FA and Tract-Specific MD

We observed sex differences that were global for FA but suggested tract-specific differences for MD. Although our initial MANOVA suggested tract-specific associations between sex and FA, these were no longer significant after controlling for global FA. Males had higher global FA values compared to females. Other studies have shown higher FA values for males compared to females, both globally and within specific tracts (Lebel et al., 2010; Inano et al., 2011; van Hemmen et al., 2017; Ritchie et al., 2018). The present results suggest that sex differences in FA are best characterized as influencing white matter integrity across the whole brain rather than within specific tracts.

In contrast, the present results suggest that sex may have tract-specific associations to MD, in which values were lower for males compared to females in the anterior cingulum and SLF, even after controlling for global MD. Higher MD in the anterior cingulum and SLF for females compared to males has previously been observed within an older adult sample (Williams et al., 2019), as well as within additional tracts that included frontal-occipital tracts, the genu, the anterior portion of the corona radiata, and the posterior limb of the internal capsule. One interpretation of our tract-specific sex differences may be that males and females are subject to a different degree of partial volume effects, given that males generally have a larger intracranial brain volume. However, if this was the case, then we would expect to see the strongest sex differences in the thinner and smaller tracts, which are more susceptible to partial volume effects. Instead, we noted sex differences in the anterior cingulum and SLF, two of the largest tracts examined in this study. An alternative interpretation is that these two tracts are particularly sensitive to alterations in female hormones because of their connections to the anterior cingulate cortex (anterior cingulum) and prefrontal cortex (SLF). Anterior cingulate cortex volume has been shown to fluctuate throughout the menstrual cycle (De Bondt et al., 2013) and shows volumetric changes with the use of hormonal contraceptives (Pletzer et al., 2010; De Bondt et al., 2013)

**TABLE 7** | Results for stepwise regressions performed on tract MD values (at time 1).

| Tract              | Predictors | $\beta$     | $t$         | $p$              | $F_{(2,46)}$ | Adj. $R^2$  | $R^2$ change |
|--------------------|------------|-------------|-------------|------------------|--------------|-------------|--------------|
| Genu*              | Global MD  | 0.80        | 9.02        | <0.001           | 41.25        | 0.63        | 0.04         |
|                    | Sex        | -0.20       | -2.24       | 0.03             |              |             |              |
| Callosum body      | Global MD  | 0.64        | 5.58        | <0.001           | 16.31        | 0.39        | 0.05         |
|                    | Sex        | -0.22       | -1.93       | n.s.             |              |             |              |
| Splenium           | Global MD  | 0.59        | 4.91        | <0.001           | 12.07        | 0.32        | 0.01         |
|                    | Sex        | -0.09       | -0.74       | n.s.             |              |             |              |
| Fornix             | Global MD  | 0.62        | 5.26        | <0.001           | 14.04        | 0.35        | 0.02         |
|                    | Sex        | -0.16       | -1.33       | n.s.             |              |             |              |
| Anterior cingulum  | Global MD  | 0.61        | 6.51        | <0.001           | <b>34.49</b> | <b>0.58</b> | <b>0.16</b>  |
|                    | <b>Sex</b> | <b>0.40</b> | <b>4.25</b> | <b>&lt;0.001</b> |              |             |              |
| Posterior cingulum | Global MD  | 0.81        | 9.27        | <0.001           | 42.99        | 0.64        | 0.01         |
|                    | Sex        | -0.10       | -1.17       | n.s.             |              |             |              |
| SLF                | Global MD  | 0.69        | 8.54        | <0.001           | <b>54.36</b> | <b>0.69</b> | <b>0.15</b>  |
|                    | <b>Sex</b> | <b>0.39</b> | <b>4.79</b> | <b>&lt;0.001</b> |              |             |              |
| IFOF               | Global MD  | 0.69        | 6.42        | <0.001           | 20.59        | 0.45        | 0.01         |
|                    | Sex        | -0.09       | -0.83       | n.s.             |              |             |              |
| Uncinate           | Global MD  | 0.70        | 6.69        | <0.001           | 23.34        | 0.48        | <0.01        |
|                    | Sex        | 0.05        | 0.47        | n.s.             |              |             |              |

Global MD was entered into each model first, followed by age. Only results for the complete model (Global MD + Sex) are included here. Standardized  $\beta$  coefficients,  $t$ -statistics, and  $p$ -values are shown for Global MD and Sex predictors. The model-level  $F$  statistic and Adj.  $R^2$  are also reported.  $R^2$  change represents the amount of variance additionally explained by the model after adding Sex as a predictor. Statistically significant sex effects are bolded (except for the genu, as removing a single outlier value rendered this effect nonsignificant).

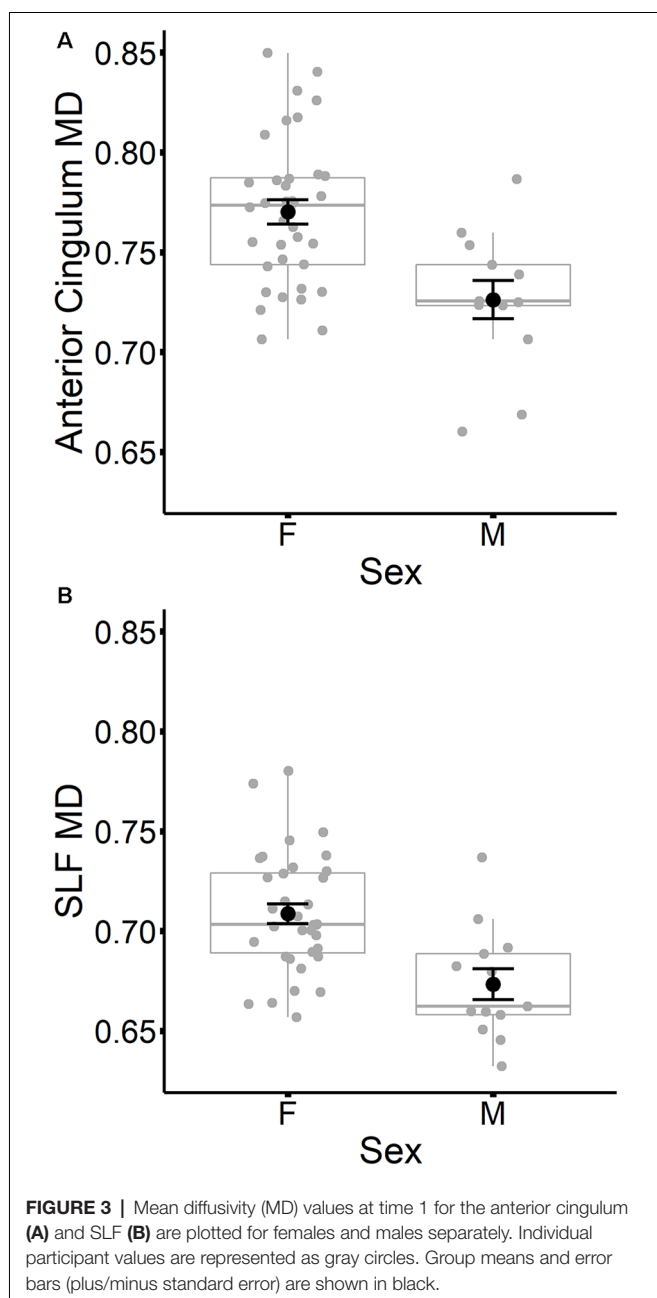
**TABLE 8** | Results of the mixed ANOVAs for global FA (left) and global MD (right) values.

| Predictors               | Global FA model |       |                | Global MD model |        |                |
|--------------------------|-----------------|-------|----------------|-----------------|--------|----------------|
|                          | $F$             | $p$   | Pillai's trace | $F$             | $p$    | Pillai's trace |
| <b>Within-subject</b>    |                 |       |                |                 |        |                |
| Time                     | 4.84            | 0.033 | 0.10           | 15.64           | <0.001 | 0.26           |
| Time * Age               | <0.001          | n.s.  | <0.01          | 0.70            | n.s.   | 0.02           |
| Time * Sex               | 1.92            | n.s.  | 0.04           | 0.01            | n.s.   | <0.01          |
| Time * APOE $\epsilon$ 4 | 0.03            | n.s.  | <0.01          | 0.27            | n.s.   | 0.01           |
| <b>Between-subject</b>   |                 |       |                |                 |        |                |
| Age                      | 9.87            | 0.003 | 0.18           | 44.73           | <0.001 | 0.50           |
| Sex                      | 11.02           | 0.002 | 0.20           | 4.03            | n.s.   | 0.08           |
| APOE $\epsilon$ 4        | 0.07            | n.s.  | <0.01          | 0.35            | n.s.   | 0.01           |

and hormone therapy (Zhang et al., 2016). Both animal and human studies suggest that estrogen regulates the activity of monoamines in the prefrontal cortex (Inagaki et al., 2010; Jacobs and D'Esposito, 2011) and that a decline in estrogen levels during menopause can have negative consequences for prefrontal cortical function (for review, see Shanmugan and Epperson, 2014). The vulnerabilities of these regions to alterations in female hormones could help account for sex differences in their associated white matter tracts. However, we did not observe sex differences in other tracts such as the fornix that also connect with hormone-sensitive limbic, hippocampal, and prefrontal areas (Catenaccio et al., 2016). Observing sex differences in smaller tracts like the fornix may require larger sample sizes than those included in the present study. While a single outlier value appeared to drive the effect of sex on the genu in our study, it is interesting to note that this result resembles observations from other studies of adult women having greater genu FA values compared to men (Oh et al., 2007; Kanaan et al., 2012, 2014).

Older women may be especially at risk for poorer white matter health due to metabolic disruptions that arise throughout menopause. Estrogen helps regulate glucose consumption

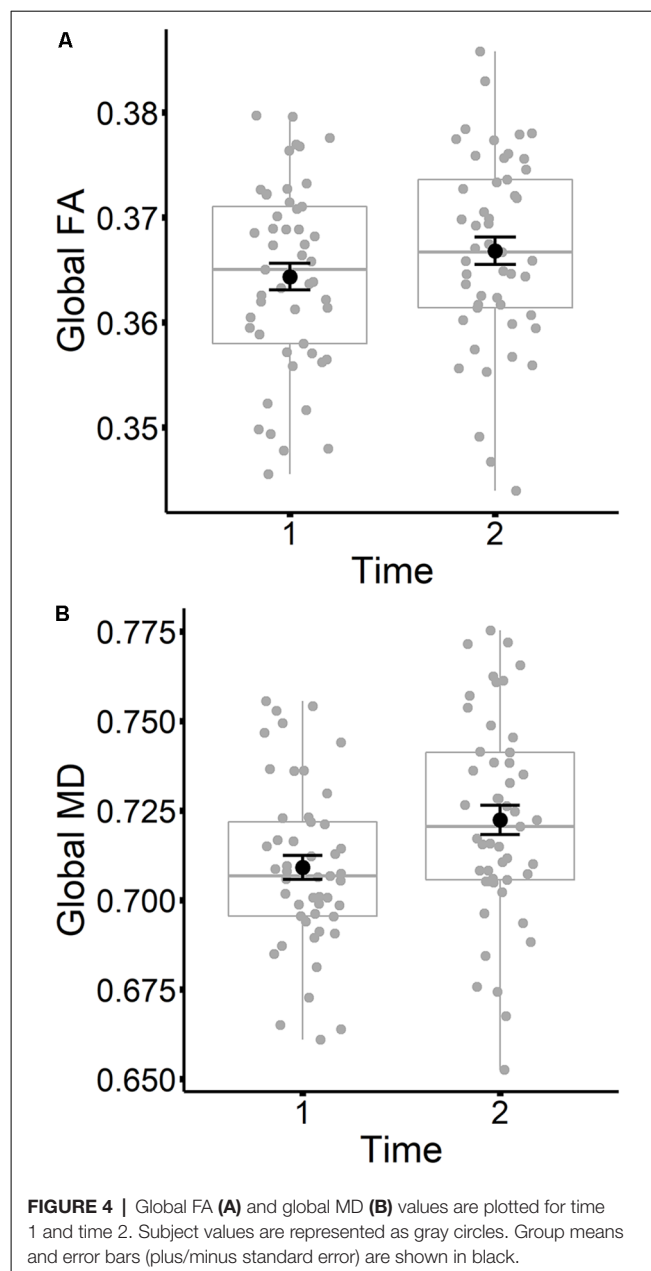
to support the maintenance of bioenergetic systems in the brain (Rettberg et al., 2014). Therefore, when estrogen production declines during menopause, glucose metabolism in the brain is likewise impaired (Brinton et al., 2015). In this hypometabolic state, the brain may compensate by utilizing ketones as an energy resource (Riedel et al., 2016) which are converted from fatty acids—including the lipids that form white matter myelin. Supporting this hypothesis, Klosinski et al. (2015) observed white matter myelin catabolization occurring in aged female mice in response to menopause-induced glucose dysfunction, with axons showing signs of extensive myelin breakdown in the post-menopausal mice. The authors suggest that this phenomenon may be adaptive for maintaining neuronal function in the face of diminished glucose utilization, although perhaps only in the short-term. In humans, white matter catabolization may render older females more susceptible to neurological diseases that feature demyelination, such as Alzheimer's Disease (Brinton et al., 2015). In the present study, we cannot say whether the sex differences we observed were due to changes associated with menopause, or reflect other differences in developmental trajectories, such as during adolescence. We view these findings



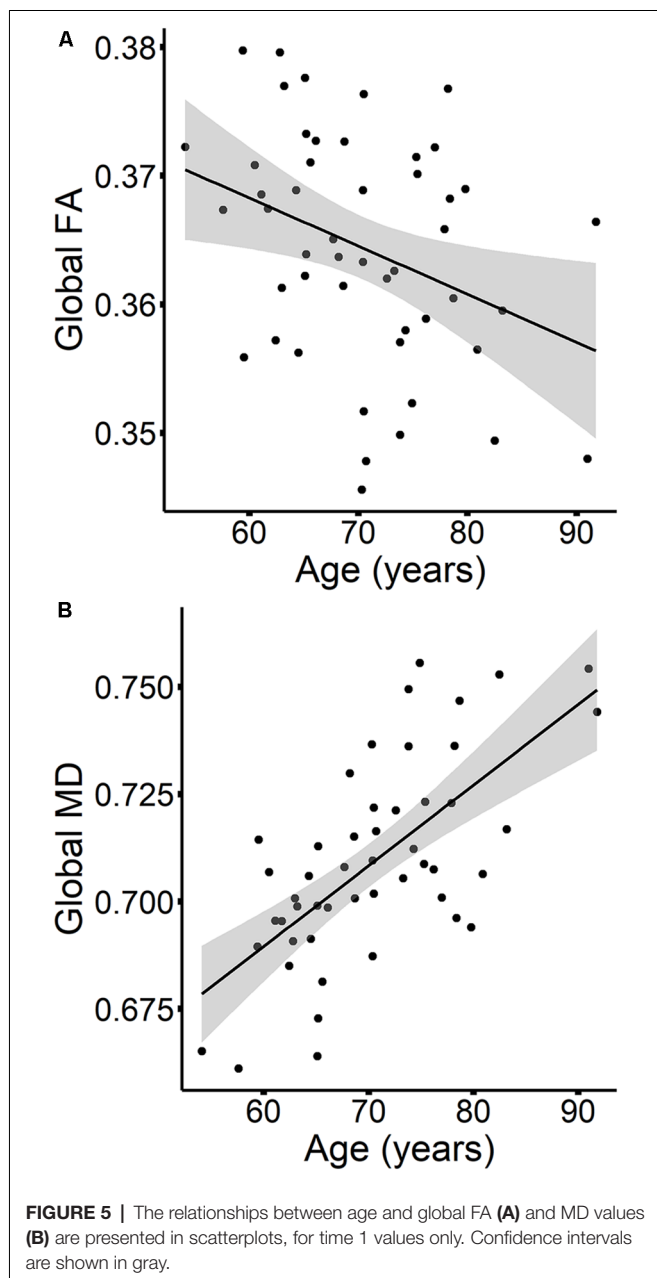
as preliminary, in part because of the low number of males included within the sample, and acknowledge the need for replication. Clearly, this is an important and promising line of research that warrants further study, ideally through the use of longitudinal designs and the inclusion of broader lifespan samples.

### Age Predicted Global MD and Both Global and Tract-Specific FA

Age exerted robust global effects on MD and both global and tract-specific effects on FA. After controlling for global MD, the impact of baseline age on tract-specific MD values was non-significant, suggesting that the effects of age on MD were

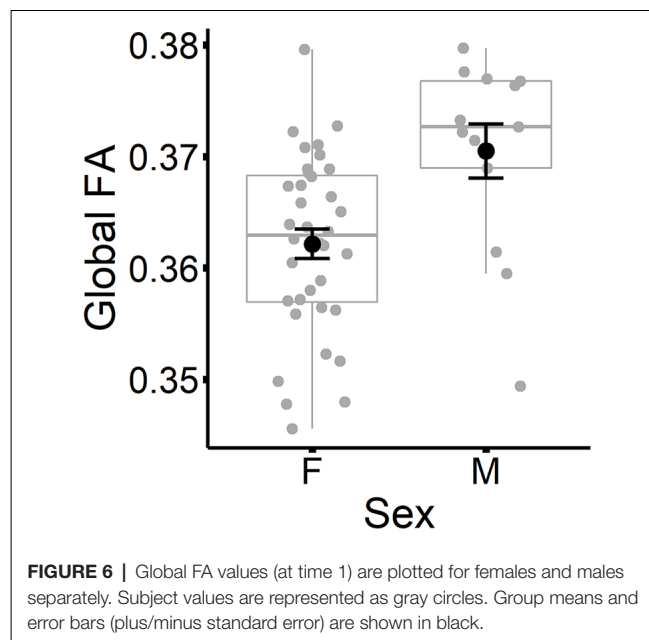


principally global, affecting white matter similarly throughout the cortex. Indeed, age alone accounted for 50% of the variance in global MD. The results for FA were more complicated. For global FA, baseline age also had a significant influence, although it accounted for a smaller portion of the variance (18%) compared to MD. Importantly, however, even after controlling for global FA, increasing age was associated with lower FA in multiple tracts including the genu and body of the corpus callosum, the anterior and posterior cingulum, and the IFOF. Age explained at minimum an additional 6% of the variance in FA values (IFOF), and up to 20% of the variance (posterior cingulum) beyond the variance explained by global FA. The results suggest that age influenced the integrity of white matter throughout the brain, but that



certain tracts may be particularly vulnerable to the effects of age-related pathologies.

The global influence of age on MD and FA values may stem from the variety of cardiovascular, metabolic, and inflammatory processes that are commonly seen in late adulthood. In particular, cardiovascular risk factors (i.e., high blood pressure, high cholesterol, obesity) have been linked to DTI alterations in late adulthood (McEvoy et al., 2015; Fuhrmann et al., 2019; Williams et al., 2019), suggesting that poor cardiovascular health relates to impaired white matter integrity among middle-aged to older adults. There is also evidence linking white matter integrity to glucose metabolic dysfunction, as DTI alterations associated with type 2 diabetes diagnosis (Reijmer et al., 2013;



Xiong et al., 2016; Sun et al., 2018; Zhuo et al., 2019) and measurably higher insulin resistance levels (Ryu et al., 2014) have been noted in studies of late adulthood. Beyond the global impact of age on white matter, the increased sensitivity of some tracts may be a consequence of variation in their structural composition. Regional differences in myelination levels have been proposed as one potential factor contributing to the differential vulnerability of white matter tracts to aging (Raz, 2000; Hoagey et al., 2019). For example, fibers in the genu are mostly thinner and less densely myelinated (Aboitiz et al., 1992; Björnholm et al., 2017) than fibers in the splenium. Multiple DTI studies have reported more robust associations between age and the genu compared to the splenium (Bendlin et al., 2010; Michielse et al., 2010; Bennett et al., 2010; Cox et al., 2016), consistent with the results of the present study.

Alternatively, it is important to consider that methodological issues may account for some of the tract-specific findings. ROI-based analyses are particularly sensitive to partial volume error, particularly in populations where atrophy is common, such as older adults. Differences in ROI size, tract size, or presence of crossing fibers can result in more or less sensitivity to partial volume error across tracts identified using *a priori* ROIs. These issues can affect the calculation of DTI metrics and artificially inflate variance among tracts. Utilizing a higher-resolution sequence, with a smaller voxel size and a greater number of diffusion gradients, would help to minimize partial volume effects in future studies. As well, replicating the present findings using alternative DTI methods including native-space fiber tracking or multivariate voxel-wise analyses that carry different advantages/disadvantages over ROI-based methods would help confirm a biological basis to these tract-specific age effects.

## Time Predicts Global Changes in MD and FA

Across the two timepoints sampled 2.7 years apart on average, we observed global changes in FA and MD. Once global DTI metrics were controlled for, there was no evidence of tract-specific changes over time. Consistent with prior research (de Groot et al., 2016; Storsve et al., 2016), we observed increases in global MD that mirrored our cross-sectional findings of a relationship between higher baseline age and elevated global MD. The lack of tract-specificity in MD changes, again consistent with our cross-sectional results, strengthens the argument that MD alterations due to aging occur in a widespread, regionally non-specific manner. Contrary to expectations and inconsistent with our cross-sectional associations with baseline age, global FA exhibited an increase over the time window. While surprising, Bender and Raz (2015) also observed similar FA increases over a two to three year period in the body of the corpus callosum across the adult lifespan and found that hypertension treatment duration moderated these changes. To our knowledge, no other study has reported age-associated increases in global FA longitudinally, and thus we take caution in interpreting this finding before replication.

The changes observed in MD and FA overtime did not vary across individuals concerning other factors included in the present study such as APOE  $\epsilon$ 4 status and sex, despite prior evidence that APOE  $\epsilon$ 4 status moderates age-related declines in DTI metrics (Ryan et al., 2011; Williams et al., 2019). Possibly, a period of 2–3 years is not sufficient to observe substantial alterations in white matter microstructural integrity associated with other moderating variables, particularly in a relatively healthy sample of older adults such as the present study. Alternatively, studies evaluating DTI metric changes over a similar length of time may require larger sample sizes, such as Bender and Raz (2015), who noted that trajectories over time were modified by health and genetic factors.

## Implications

In summary, we found that age exerts a strongly negative influence on white matter microstructural health that is widespread among association, limbic, and commissural tracts. However, there is considerable variation in the extent to which these tracts are affected by age, with some like the posterior cingulum more severely affected than others like the IFOF. We also observed poorer white matter health in females relative to males. The results of this study highlight the importance of considering global white matter when attempting to understand how predictive factors such as age, sex, or APOE  $\epsilon$ 4 status influence DTI metrics. Findings that initially appeared to be tract-specific, such as the effect of sex on FA, arose because of a strong association between the

predictor and global white matter FA. Considering the impact of aging on FA, controlling for global FA was important in allowing us to more precisely characterize the sensitivity of individual tracts to age-related damage. Though not a standard practice, other DTI studies have similarly controlled for global DTI metrics to ensure the specificity of relationships between tract integrity and outcome measures by deriving the mean of DTI values across white matter (Bennett et al., 2015; Ngo et al., 2017; Memel et al., 2020), the mean of DTI values across the tracts of interest (Rabin et al., 2019), or a general factor of variance shared across tracts of interest (Penke et al., 2010; Cox et al., 2016). The results of the present study suggest that it may be important to account for global white matter DTI values when examining tract-specific associations between DTI metrics and variables such as age, sex, or APOE genotype. Future studies will be needed to replicate our results, ideally employing different methods and analytic approaches, to determine the strengths of each for determining the factors that influence global and tract-specific white matter variation.

## DATA AVAILABILITY STATEMENT

The raw data supporting the conclusions of this article will be made available by the authors, without undue reservation.

## ETHICS STATEMENT

The studies involving human participants were reviewed and approved by University of Arizona's Institutional Review Board. The patients/participants provided their written informed consent to participate in this study.

## AUTHOR CONTRIBUTIONS

SM and LR designed the study, wrote, revised and approved the submitted manuscript. SM processed imaging data and performed the statistical analyses. All authors contributed to the article and approved the submitted version.

## FUNDING

This work was supported by the Arizona Alzheimer's Research Consortium, Arizona Department of Health Services. SM was funded by National Science Foundation Graduate Research Fellowship Grant DGE-1746060.

## ACKNOWLEDGMENTS

We thank our participants for their generous help in our study.

## REFERENCES

Aboitiz, F., Scheibel, A. B., Fisher, R. S., and Zaidel, E. (1992). Fiber composition of the human corpus callosum. *Brain Res.* 598, 143–153. doi: 10.1016/0006-8993(92)90178-c

Adluru, N., Destiche, D. J., Lu, S. Y.-F., Doran, S. T., Birdsill, A. C., Melah, K. E., et al. (2014). White matter microstructure in late middle-age: effects of apolipoprotein E4 and parental family history of Alzheimer's disease. *NeuroImage Clin.* 4, 730–742. doi: 10.1016/j.nicl.2014.04.008

- Alexander, A. L., Lee, J. E., Lazar, M., and Field, A. S. (2007). Diffusion tensor imaging of the brain. *Neurotherapeutics* 4, 316–329. doi: 10.1016/j.nurt.2007.05.011
- Bender, A. R., and Raz, N. (2015). Normal-appearing cerebral white matter in healthy adults: mean change over 2 years and individual differences in change. *Neurobiol. Aging* 36, 1834–1848. doi: 10.1016/j.neurobiolaging.2015.02.001
- Bender, A. R., Völkle, M. C., and Raz, N. (2016). Differential aging of cerebral white matter in middle-aged and older adults: a seven-year follow-up. *NeuroImage* 125, 74–83. doi: 10.1016/j.neuroimage.2015.10.030
- Bendlin, B. B., Ries, M. L., Canu, E., Sodhi, A., Lazar, M., Alexander, A. L., et al. (2010). White matter is altered with parental family history of Alzheimer's disease. *Alzheimers Dement.* 6, 394–403. doi: 10.1016/j.jalz.2009.11.003
- Bennett, I. J., Huffman, D. J., and Stark, C. E. (2015). Limbic tract integrity contributes to pattern separation performance across the lifespan. *Cereb. Cortex* 25, 2988–2999. doi: 10.1093/cercor/bhu093
- Bennett, I. J., Madden, D. J., Vaidya, C. J., Howard, D. V., and Howard, J. H. Jr. (2010). Age related differences in multiple measures of white matter integrity: a diffusion tensor imaging study of healthy aging. *Hum. Brain Mapp.* 31, 378–390. doi: 10.1002/hbm.20872
- Björnholm, L., Nikkinen, J., Kiviniemi, V., Nordström, T., Niemelä, S., Drakesmith, M., et al. (2017). Structural properties of the human corpus callosum: multimodal assessment and sex differences. *NeuroImage* 152, 108–118. doi: 10.1016/j.neuroimage.2017.02.056
- Brickman, A. M., Meier, I. B., Korgaonkar, M. S., Provenzano, F. A., Grieve, S. M., Siedlecki, K. L., et al. (2012). Testing the white matter retrogenesis hypothesis of cognitive aging. *Neurobiol. Aging* 33, 1699–1715. doi: 10.1016/j.neurobiolaging.2011.06.001
- Brinton, R. D., Yao, J., Yin, F., Mack, W. J., and Cadenas, E. (2015). Perimenopause as a neurological transition state. *Nat. Rev. Endocrinol.* 11, 393–405. doi: 10.1038/nrendo.2015.82
- Budde, M. D., Kim, J. H., Liang, H., Schmidt, R. E., Russell, J. H., Cross, A. H., et al. (2007). Toward accurate diagnosis of white matter pathology using diffusion tensor imaging. *Magn. Reson. Med.* 57, 688–695. doi: 10.1002/mrm.21200
- Budde, M. D., Xie, M., Cross, A. H., and Song, S.-K. (2009). Axial diffusivity is the primary correlate of axonal injury in the experimental autoimmune encephalomyelitis spinal cord: a quantitative pixelwise analysis. *J. Neurosci.* 29, 2805–2813. doi: 10.1523/JNEUROSCI.4605-08.2009
- Burzynska, A. Z., Preuschhof, C., Bäckman, L., Nyberg, L., Li, S.-C., Lindenberger, U., et al. (2010). Age-related differences in white matter microstructure: region-specific patterns of diffusivity. *NeuroImage* 49, 2104–2112. doi: 10.1016/j.neuroimage.2009.09.041
- Catenaccio, E., Mu, W., and Lipton, M. L. (2016). Estrogen- and progesterone-mediated structural neuroplasticity in women: evidence from neuroimaging. *Brain Struct. Funct.* 221, 3845–3867. doi: 10.1007/s00429-016-1197-x
- Cavedo, E., Lista, S., Rojkova, K., Chiesa, P. A., Houot, M., Brueggen, K., et al. (2017). Disrupted white matter structural networks in healthy older adult APOE  $\epsilon 4$  carriers—an international multicenter DTI study. *Neuroscience* 357, 119–133. doi: 10.1016/j.neuroscience.2017.05.048
- Chapman, T. W., and Hill, R. A. (2020). Myelin plasticity in adulthood and aging. *Neurosci. Lett.* 715:134645. doi: 10.1016/j.neulet.2019.134645
- Cox, S. R., Ritchie, S. J., Tucker-Drob, E. M., Liewald, D. C., Hagenaars, S. P., Davies, G., et al. (2016). Ageing and brain white matter structure in 3,513 UK Biobank participants. *Nat. Commun.* 7:13629. doi: 10.1038/ncomms13629
- De Bondt, T., Jacquemyn, Y., Van Hecke, W., Sijbers, J., Sunaert, S., and Parizel, P. M. (2013). Regional gray matter volume differences and sex-hormone correlations as a function of menstrual cycle phase and hormonal contraceptives use. *Brain Res.* 1530, 22–31. doi: 10.1016/j.brainres.2013.07.034
- de Groot, M., Cremers, L. G. M., Ikram, M. A., Hofman, A., Krestin, G. P., van der Lugt, A., et al. (2016). White matter degeneration with aging: longitudinal diffusion MR imaging analysis. *Radiology* 279, 532–541. doi: 10.1148/radiol.2015150103
- de Groot, M., Ikram, M. A., Akoudad, S., Krestin, G. P., Hofman, A., Van Der Lugt, A., et al. (2015). Tract-specific white matter degeneration in aging: the Rotterdam study. *Alzheimers Dement.* 11, 321–330. doi: 10.1016/j.jalz.2014.06.011
- Desai, M. K., and Brinton, R. D. (2019). Autoimmune disease in women: endocrine transition and risk across the lifespan. *Front. Endocrinol.* 10:265. doi: 10.3389/fendo.2019.00265
- Falangola, M. F., Guilfoyle, D. N., Tabesh, A., Hui, E. S., Nie, X., Jensen, J. H., et al. (2014). Histological correlation of diffusional kurtosis and white matter modeling metrics in cuprizone-induced corpus callosum demyelination. *NMR Biomed.* 27, 948–957. doi: 10.1002/nbm.3140
- Fuhrmann, D., Nesbitt, D., Shafto, M., Rowe, J. B., Price, D., Gadie, A., et al. (2019). Strong and specific associations between cardiovascular risk factors and white matter micro- and macrostructure in healthy aging. *Neurobiol. Aging* 74, 46–55. doi: 10.1016/j.neurobiolaging.2018.10.005
- Gustavson, D. E., Hatton, S. N., Elman, J. A., Panizzon, M. S., Franz, C. E., Hagler, D. J., et al. (2019). Predominantly global genetic influences on individual white matter tract microstructure. *NeuroImage* 184, 871–880. doi: 10.1016/j.neuroimage.2018.10.016
- Hatton, S. N., Panizzon, M. S., Vuoksimaa, E., Hagler, D. J., Fennema-Notestine, C., Rinker, D., et al. (2018). Genetic relatedness of axial and radial diffusivity indices of cerebral white matter microstructure in late middle age. *Hum. Brain Mapp.* 39, 2235–2245. doi: 10.1002/hbm.24002
- Heise, V., Filippini, N., Ebmeier, K. P., and Mackay, C. E. (2011). The APOE $\epsilon 4$  allele modulates brain white matter integrity in healthy adults. *Mol. Psychiatry* 16, 908–916. doi: 10.1038/mp.2010.90
- Herting, M. M., Maxwell, E. C., Irvine, C., and Nagel, B. J. (2012). The impact of sex, puberty and hormones on white matter microstructure in adolescents. *Cereb. Cortex* 22, 1979–1992. doi: 10.1093/cercor/bhr246
- Ho, T. C., Colich, N. L., Sisk, L. M., Oskirko, K., Jo, B., and Gotlib, I. H. (2020). Sex differences in the effects of gonadal hormones on white matter microstructure development in adolescence. *Dev. Cogn. Neurosci.* 42:100773. doi: 10.1016/j.dcn.2020.100773
- Hoagey, D. A., Rieck, J. R., Rodrigue, K. M., and Kennedy, K. M. (2019). Joint contributions of cortical morphometry and white matter microstructure in healthy brain aging: a partial least squares correlation analysis. *Hum. Brain Mapp.* 40, 5315–5329. doi: 10.1002/hbm.24774
- Inagaki, T., Gautreaux, C., and Luine, V. (2010). Acute estrogen treatment facilitates recognition memory consolidation and alters monoamine levels in memory-related brain areas. *Horm. Behav.* 58, 415–426. doi: 10.1016/j.yhbeh.2010.05.013
- Inano, S., Takao, H., Hayashi, N., Abe, O., and Ohtomo, K. (2011). Effects of age and gender on white matter integrity. *Am. J. Neuroradiol.* 32, 2103–2109. doi: 10.3174/ajnr.A2785
- Jacobs, E., and D'Esposito, M. (2011). Estrogen shapes dopamine-dependent cognitive processes: implications for women's health. *J. Neurosci.* 31, 5286–5293. doi: 10.1523/JNEUROSCI.6394-10.2011
- Kanaan, R. A., Allin, M., Picchioni, M., Barker, G. J., Daly, E., Shergill, S. S., et al. (2012). Gender differences in white matter microstructure. *PLoS One* 7:e38272. doi: 10.1371/journal.pone.0038272
- Kanaan, R. A., Chaddock, C., Allin, M., Picchioni, M. M., Daly, E., Shergill, S. S., et al. (2014). Gender influence on white matter microstructure: a tract-based spatial statistics analysis. *PLoS One* 9:e91109. doi: 10.1371/journal.pone.0091109
- Kanchibhotla, S. C., Mather, K. A., Thalamuthu, A., Zhuang, L., Schofield, P. R., Kwok, J. B. J., et al. (2014). Genetics of microstructure of the corpus callosum in older adults. *PLoS One* 9:e113181. doi: 10.1371/journal.pone.0113181
- Kanchibhotla, S. C., Mather, K. A., Wen, W., Schofield, P. R., Kwok, J. B. J., and Sachdev, P. S. (2013). Genetics of ageing-related changes in brain white matter integrity—a review. *Ageing Res. Rev.* 12, 391–401. doi: 10.1016/j.arr.2012.10.003
- Karim, R., Koc, M., Rettberg, J. R., Hodis, H. N., Henderson, V. W., St John, J. A., et al. (2019). Apolipoprotein E4 genotype in combination with poor metabolic profile is associated with reduced cognitive performance in healthy postmenopausal women: implications for late onset Alzheimer's disease. *Menopause* 26, 7–15. doi: 10.1097/GME.0000000000001160
- Keihaninejad, S., Zhang, H., Ryan, N. S., Malone, I. B., Modat, M., Cardoso, M. J., et al. (2013). An unbiased longitudinal analysis framework for tracking white matter changes using diffusion tensor imaging with application to Alzheimer's disease. *NeuroImage* 72, 153–163. doi: 10.1016/j.neuroimage.2013.01.044
- Kline, A. (2012). Apolipoprotein E, amyloid- $\beta$  clearance and therapeutic opportunities in Alzheimer's disease. *Alzheimers Res. Ther.* 4:32. doi: 10.1186/alzrt135

- Klosinski, L. P., Yao, J., Yin, F., Fonteh, A. N., Harrington, M. G., Christensen, T. A., et al. (2015). White matter lipids as a ketogenic fuel supply in aging female brain: implications for Alzheimer's disease. *EBioMedicine* 2, 1888–1904. doi: 10.1016/j.ebiom.2015.11.002
- Laukka, E. J., Lövdén, M., Kalpouzos, G., Papenberg, G., Keller, L., Graff, C., et al. (2015). Microstructural white matter properties mediate the association between APOE and perceptual speed in very old persons without dementia. *PLoS One* 10:e0134766. doi: 10.1371/journal.pone.0134766
- Lebel, C., Caverhill-Godkewitch, S., and Beaulieu, C. (2010). Age-related regional variations of the corpus callosum identified by diffusion tensor tractography. *NeuroImage* 52, 20–31. doi: 10.1016/j.neuroimage.2010.03.072
- Lebel, C., Gee, M., Camicioli, R., Wieler, M., Martin, W., and Beaulieu, C. (2012). Diffusion tensor imaging of white matter tract evolution over the lifespan. *NeuroImage* 60, 340–352. doi: 10.1016/j.neuroimage.2011.11.094
- Lindenberger, U., Nagel, I. E., Chicherio, C., Li, S.-C., Heekeren, H. R., and Bäckman, L. (2008). Age-related decline in brain resources modulates genetic effects on cognitive functioning. *Front. Neurosci.* 2, 234–244. doi: 10.3389/neuro.01.039.2008
- Lövdén, M., Laukka, E. J., Rieckmann, A., Kalpouzos, G., Li, T.-Q., Jonsson, T., et al. (2013). The dimensionality of between-person differences in white matter microstructure in old age. *Hum. Brain Mapp.* 34, 1386–1398. doi: 10.1002/hbm.21518
- Ly, M., Canu, E., Xu, G., Oh, J., McLaren, D. G., Dowling, N. M., et al. (2014). Midlife measurements of white matter microstructure predict subsequent regional white matter atrophy in healthy adults. *Hum. Brain Mapp.* 35, 2044–2054. doi: 10.1002/hbm.22311
- Lyall, D. M., Harris, S. E., Bastin, M. E., Muñoz Maniega, S., Murray, C., Lutz, M. W., et al. (2014). Alzheimer's disease susceptibility genes APOE and TOMM40 and brain white matter integrity in the Lothian Birth Cohort 1936. *Neurobiol. Aging* 35, 1513.e25–1513.e25. doi: 10.1016/j.neurobiolaging.2014.01.006
- Madden, D. J., Bennett, I. J., and Song, A. W. (2009). Cerebral white matter integrity and cognitive aging: contributions from diffusion tensor imaging. *Neuropsychol. Rev.* 19, 415–435. doi: 10.1007/s11065-009-9113-2
- Marstaller, L., Williams, M., Rich, A., Savage, G., and Burianova, H. (2015). Aging and large-scale functional networks: white matter integrity, gray matter volume, and functional connectivity in the resting state. *Neuroscience* 290, 369–378. doi: 10.1016/j.neuroscience.2015.01.049
- McEvoy, L. K., Fennema-Notestine, C., Eyler, L. T., Franz, C. E., Hagler, D. J. Jr., Lyons, M. J., et al. (2015). Hypertension-related alterations in white matter microstructure detectable in middle age. *Hypertension* 66, 317–323. doi: 10.1161/HYPERTENSIONAHA.115.05336
- Memel, M., Wank, A. A., Ryan, L., and Grilli, M. D. (2020). The relationship between episodic detail generation and anterotemporal, posteromedial, and hippocampal white matter tracts. *Cortex* 123, 124–140. doi: 10.1016/j.cortex.2019.10.010
- Menzies, L., Goddings, A.-L., Whitaker, K. J., Blakemore, S.-J., and Viner, R. M. (2015). The effects of puberty on white matter development in boys. *Dev. Cogn. Neurosci.* 11, 116–128. doi: 10.1016/j.dcn.2014.10.002
- Michiels, S., Coupland, N., Camicioli, R., Carter, R., Seres, P., Sabino, J., et al. (2010). Selective effects of aging on brain white matter microstructure: a diffusion tensor imaging tractography study. *NeuroImage* 52, 1190–1201. doi: 10.1016/j.neuroimage.2010.05.019
- Mori, S., Oishi, K., Jiang, H., Jiang, L., Li, X., Akhter, K., et al. (2008). Stereotaxic white matter atlas based on diffusion tensor imaging in an ICBM template. *NeuroImage* 40, 570–582. doi: 10.1016/j.neuroimage.2007.12.035
- Mosconi, L., Berti, V., Quinn, C., McHugh, P., Petrongolo, G., Varsavsky, I., et al. (2017). Sex differences in Alzheimer risk: brain imaging of endocrine vs chronologic aging. *Neurology* 89, 1382–1390. doi: 10.1212/WNL.0000000000004425
- Ngo, C. T., Alm, K. H., Metoki, A., Hampton, W., Riggins, T., Newcombe, N. S., et al. (2017). White matter structural connectivity and episodic memory in early childhood. *Dev. Cogn. Neurosci.* 28, 41–53. doi: 10.1016/j.dcn.2017.11.001
- Nyberg, L., and Salami, A. (2014). The APOE  $\epsilon$  4 allele in relation to brain white-matter microstructure in adulthood and aging. *Scand. J. Psychol.* 55, 263–267. doi: 10.1111/sjop.12099
- O'Donnell, L. J., and Westin, C. F. (2011). An introduction to diffusion tensor image analysis. *Neurosurg. Clin. N. Am.* 22, 185–196, viii. doi: 10.1016/j.nec.2010.12.004
- O'Dwyer, L., Lamberton, F., Bokde, A. L. W., Ewers, M., Faluy, Y. O., Tanner, C., et al. (2012). Sexual dimorphism in healthy aging and mild cognitive impairment: a DTI study. *PLoS One* 7:e37021. doi: 10.1371/journal.pone.0037021
- Oh, J. S., Song, I. C., Lee, J. S., Kang, H., Park, K. S., Kang, E., et al. (2007). Tractography-guided statistics (TGIS) in diffusion tensor imaging for the detection of gender difference of fiber integrity in the midsagittal and parasagittal corpora callosa. *NeuroImage* 36, 606–616. doi: 10.1016/j.neuroimage.2007.03.020
- Papenberg, G., Lindenberger, U., and Bäckman, L. (2015). Aging-related magnification of genetic effects on cognitive and brain integrity. *Trends Cogn. Sci.* 19, 506–514. doi: 10.1016/j.tics.2015.06.008
- Penke, L., Muñoz Maniega, S., Murray, C., Gow, A. J., Valdés Hernández, M. C., Clayden, J. D., et al. (2010). A general factor of brain white matter integrity predicts information processing speed in healthy older people. *J. Neurosci.* 30, 7569–7574. doi: 10.1523/JNEUROSCI.1553-10.2010
- Peper, J. S., De Reus, M. A., Van Den Heuvel, M. P., and Schutter, D. J. L. G. (2015). Short fused? associations between white matter connections, sex steroids and aggression across adolescence. *Hum. Brain Mapp.* 36, 1043–1052. doi: 10.1002/hbm.22684
- Persson, J., Lind, J., Larsson, A., Ingvar, M., Cruts, M., Van Broeckhoven, C., et al. (2006). Altered brain white matter integrity in healthy carriers of the APOE  $\epsilon$  4 allele: a risk for AD? *Neurology* 66, 1029–1033. doi: 10.1212/01.wnl.0000204180.25361.48
- Peters, A. (2009). The effects of normal aging on myelinated nerve fibers in monkey central nervous system. *Front. Neuroanat.* 3:11. doi: 10.3389/neuro.05.011.2009
- Pletzer, B., Kronbichler, M., Aichhorn, M., Bergmann, J., Ladurner, G., and Kerschbaum, H. H. (2010). Menstrual cycle and hormonal contraceptive use modulate human brain structure. *Brain Res.* 1348, 55–62. doi: 10.1016/j.brainres.2010.06.019
- Rabin, J. S., Perea, R. D., Buckley, R. F., Neal, T. E., Buckner, R. L., Johnson, K. A., et al. (2019). Global white matter diffusion characteristics predict longitudinal cognitive change independently of amyloid status in clinically normal older adults. *Cereb. Cortex* 29, 1251–1262. doi: 10.1093/cercor/bhy031
- Raj, D., Yin, Z., Breur, M., Doorduyn, J., Holtman, I. R., Olah, M., et al. (2017). Increased white matter inflammation in aging- and Alzheimer's disease brain. *Front. Mol. Neurosci.* 10:206. doi: 10.3389/fnmol.2017.00206
- Raz, N. (2000). "Aging of the brain and its impact on cognitive performance: integration of structural and functional findings," in *The Handbook of Aging and Cognition*, eds F. I. M. Craik and T. A. Salthouse (New Jersey, NJ: Lawrence Erlbaum Associates Publishers), 1–90.
- Reijmer, Y. D., Brundel, M., de Bresser, J., Kappelle, L. J., Leemans, A., Biessels, G. J., et al. (2013). Microstructural white matter abnormalities and cognitive functioning in type 2 diabetes: a diffusion tensor imaging study. *Diabetes Care* 36, 137–144. doi: 10.2337/dc12-0493
- Rettberg, J. R., Yao, J., and Brinton, R. D. (2014). Estrogen: a master regulator of bioenergetic systems in the brain and body. *Front. Neuroendocrinol.* 35, 8–30. doi: 10.1016/j.yfrne.2013.08.001
- Rieckmann, A., Van Dijk, K. R. A., Sperling, R. A., Johnson, K. A., Buckner, R. L., and Hedden, T. (2016). Accelerated decline in white matter integrity in clinically normal individuals at risk for Alzheimer's disease. *Neurobiol. Aging* 42, 177–188. doi: 10.1016/j.neurobiolaging.2016.03.016
- Riedel, B. C., Thompson, P. M., and Brinton, R. D. (2016). Age, APOE and sex: triad of risk of Alzheimer's disease. *J. Steroid Biochem. Mol. Biol.* 160, 134–147. doi: 10.1016/j.jsbmb.2016.03.012
- Ritchie, S. J., Cox, S. R., Shen, X., Lombardo, M. V., Reus, L. M., Alloza, C., et al. (2018). Sex differences in the adult human brain: evidence from 5216 UK biobank participants. *Cereb. Cortex* 28, 2959–2975. doi: 10.1093/cercor/bhy109
- Ryan, L., Walther, K., Bendlin, B. B., Lue, L., Walker, D. G., and Glisky, E. L. (2011). Age-related differences in white matter integrity and cognitive function are related to APOE status. *NeuroImage* 54, 1565–1577. doi: 10.1016/j.neuroimage.2010.08.052

- Ryu, S. Y., Coutu, J.-P., Rosas, H. D., and Salat, D. H. (2014). Effects of insulin resistance on white matter microstructure in middle-aged and older adults. *Neurology* 82, 1862–1870. doi: 10.1212/WNL.0000000000000452
- Sexton, C. E., Walhovd, K. B., Storsve, A. B., Tamnes, C. K., Westlye, L. T., Johansen-Berg, H., et al. (2014). Accelerated changes in white matter microstructure during aging: a longitudinal diffusion tensor imaging study. *J. Neurosci.* 34, 15425–15436. doi: 10.1523/JNEUROSCI.0203-14.2014
- Shanmugan, S., and Epperson, C. N. (2014). Estrogen and the prefrontal cortex: towards a new understanding of estrogen's effects on executive functions in the menopause transition. *Hum. Brain Mapp.* 35, 847–865. doi: 10.1002/hbm.22218
- Smith, C. D., Chebrolu, H., Andersen, A. H., Powell, D. A., Lovell, M. A., Xiong, S., et al. (2010). White matter diffusion alterations in normal women at risk of Alzheimer's disease. *Neurobiol. Aging* 31, 1122–1131. doi: 10.1016/j.neurobiolaging.2008.08.006
- Smith, S. M., Jenkinson, M., Woolrich, M. W., Beckmann, C. F., Behrens, T. E. J., Johansen-Berg, H., et al. (2004). Advances in functional and structural MR image analysis and implementation as FSL. *NeuroImage* 23, S208–S219. doi: 10.1016/j.neuroimage.2004.07.051
- Song, S.-K., Sun, S.-W., Ju, W.-K., Lin, S.-J., Cross, A. H., and Neufeld, A. H. (2003). Diffusion tensor imaging detects and differentiates axon and myelin degeneration in mouse optic nerve after retinal ischemia. *NeuroImage* 20, 1714–1722. doi: 10.1016/j.neuroimage.2003.07.005
- Song, S.-K., Yoshino, J., Le, T. Q., Lin, S.-J., Sun, S.-W., Cross, A. H., et al. (2005). Demyelination increases radial diffusivity in corpus callosum of mouse brain. *NeuroImage* 26, 132–140. doi: 10.1016/j.neuroimage.2005.01.028
- Storsve, A. B., Fjell, A. M., Yendiki, A., and Walhovd, K. B. (2016). Longitudinal changes in white matter tract integrity across the adult lifespan and its relation to cortical thinning. *PLoS One* 11:e0156770. doi: 10.1371/journal.pone.0156770
- Sun, Q., Chen, G.-Q., Wang, X.-B., Yu, Y., Hu, Y.-C., Yan, L.-F., et al. (2018). Alterations of white matter integrity and hippocampal functional connectivity in type 2 diabetes without mild cognitive impairment. *Front. Neuroanat.* 12:21. doi: 10.3389/fnana.2018.00021
- Teipel, S. J., Meindl, T., Wagner, M., Stieltjes, B., Reuter, S., Hauenstein, K.-H., et al. (2010). Longitudinal changes in fiber tract integrity in healthy aging and mild cognitive impairment: a DTI follow-up study. *J. Alzheimers Dis.* 22, 507–522. doi: 10.3233/JAD-2010-100234
- van Hemmen, J., Saris, I. M. J., Cohen-Kettenis, P. T., Veltman, D. J., Pouwels, P. J. W., and Bakker, J. (2017). Sex differences in white matter microstructure in the human brain predominantly reflect differences in sex hormone exposure. *Cereb. Cortex* 27, 2994–3001. doi: 10.1093/cercor/bhw156
- Vuoksima, E., Panizzon, M. S., Hagler, D. J., Hatton, S. N., Fennema-Notestine, C., Rinker, D., et al. (2017). Heritability of white matter microstructure in late middle age: a twin study of tract-based fractional anisotropy and absolute diffusivity indices. *Hum. Brain Mapp.* 38, 2026–2036. doi: 10.1002/hbm.23502
- Westlye, L. T., Reinvang, I., Rootwelt, H., and Espeseth, T. (2012). Effects of APOE on brain white matter microstructure in healthy adults. *Neurology* 79, 1961–1969. doi: 10.1212/WNL.0b013e3182735c9c
- Williams, O. A., An, Y., Beason-Held, L., Huo, Y., Ferrucci, L., Landman, B. A., et al. (2019). Vascular burden and APOE  $\epsilon$ 4 are associated with white matter microstructural decline in cognitively normal older adults. *NeuroImage* 188, 572–583. doi: 10.1016/j.neuroimage.2018.12.009
- Winkleski, P. J., Sabisz, A., Naumczyk, P., Jodzio, K., Szurawska, E., and Szarmach, A. (2018). Understanding the physiopathology behind axial and radial diffusivity changes—what do we know? *Front. Neurol.* 9:92. doi: 10.3389/fneur.2018.00092
- Xiong, Y., Sui, Y., Xu, Z., Zhang, Q., Karaman, M. M., Cai, K., et al. (2016). A diffusion tensor imaging study on white matter abnormalities in patients with type 2 diabetes using tract-based spatial statistics. *Am. J. Neuroradiol.* 37, 1462–1469. doi: 10.3174/ajnr.A4740
- Zhang, T., Casanova, R., Resnick, S. M., Manson, J. A. E., Baker, L. D., Padual, C. B., et al. (2016). Effects of hormone therapy on brain volumes changes of postmenopausal women revealed by optimally-discriminative voxel-based morphometry. *PLoS One* 11:e0150834. doi: 10.1371/journal.pone.0150834
- Zhang, H., Yushkevich, P. A., Alexander, D. C., and Gee, J. C. (2006). Deformable registration of diffusion tensor MR images with explicit orientation optimization. *Med. Image Anal.* 10, 764–785. doi: 10.1016/j.media.2006.06.004
- Zhuo, Y., Fang, F., Lu, L., Li, T., Lian, J., Xiong, Y., et al. (2019). White matter impairment in type 2 diabetes mellitus with and without microvascular disease. *NeuroImage Clin.* 24:101945. doi: 10.1016/j.nicl.2019.101945

**Conflict of Interest:** The authors declare that the research was conducted in the absence of any commercial or financial relationships that could be construed as a potential conflict of interest.

Copyright © 2021 Matijevic and Ryan. This is an open-access article distributed under the terms of the Creative Commons Attribution License (CC BY). The use, distribution or reproduction in other forums is permitted, provided the original author(s) and the copyright owner(s) are credited and that the original publication in this journal is cited, in accordance with accepted academic practice. No use, distribution or reproduction is permitted which does not comply with these terms.